Knowledge Acquisition Method Based on Singular Value Decomposition for Human Motion Analysis

Yinlai Jiang, *Member, IEEE*, Isao Hayashi, *Member, IEEE*, and Shuoyu Wang, *Member, IEEE*

Abstract—The knowledge remembered by the human body and reflected by the dexterity of body motion is called embodied knowledge. In this paper, we propose a new method using singular value decomposition for extracting embodied knowledge from the time-series data of the motion. We compose a matrix from the time-series data and use the left singular vectors of the matrix as the patterns of the motion and the singular values as a scalar, by which each corresponding left singular vector affects the matrix. Two experiments were conducted to validate the method. One is a gesture recognition experiment in which we categorize gesture motions by two kinds of models with indexes of similarity and estimation that use left singular vectors. The proposed method obtained a higher correct categorization ratio than principal component analysis (PCA) and correlation efficiency (CE). The other is an ambulation evaluation experiment in which we distinguished the levels of walking disability. The first singular values derived from the walking acceleration were suggested to be a reliable criterion to evaluate walking disability. Finally we discuss the characteristic and significance of the embodied knowledge extraction using the singular value decomposition proposed in this paper.

Index Terms—Singular value decomposition, embodied knowledge, motion analysis, gesture recognition, walking difficulty evaluation

1 Introduction

The motions of the human body are being actively studied in the fields of medical care, sports, arts, and so on. The skill ability internalized in the body, which is called embodied knowledge or tacit knowledge, plays an important role in acquiring skills that enable, for example, athletes to move economically [1], martial artists to make more flexible movements [2], and musicians to perform with uplifting feeling [3], [4]. Embodied knowledge is a native human endowment that is usually not consciously accessible.

Embodied knowledge has been studied from the viewpoint of not only neurophysiology, but also the structure of the body. Miall et al. proposed a forward model to output a signal to a controlled object via feedback control using the Smith predictor having no time delay for the control [5], [6]. Kawato proposed a cerebellar computational model, called an internal model, which argued that the inverse model with feedback and feedforward control is useful in modeling motor control [7], [8]. The forward and inverse models are remarkable in constituting an internal model. Instead of arguing about internal model construction, we propose identifying the relationship between sensor input and the output of internal model movement as knowledge. Our approach assumes that skills consist of a hierarchical structure with a mono-functional layer to generate the single function result and a meta-functional layer that adapts itself to environmental change, as shown in Fig. 1. We assume that a skill is the knowledge embodied in the human body.

The information of motion, such as trajectory, speed, and acceleration, has been measured to extract and analyze embodied knowledge [3], [4], [9], [10], [11], [12], [13], [14], [15]. Time-series data analysis is usually necessary to extract features from the measurement data. Various methods for analyzing physical movement have been proposed. Mitra and Acharya [16] surveyed varied methods for gesture recognition, ranging from mathematical models, such as hidden Markov models (HMMs) and particle filter, to soft computing approaches such as artificial neural network and fuzzy sets. Wilson and Bobick [17] proposed parametric HMMs which outperformed standard HMMs in an experiment to recognize three-dimensional hand gestures. Pylvanainen [18] presented a gesture recognition system based on continuous HMMs to recognize gestures measured by a 3D accelerometer. Lichtenauer et al. [19] recognized sign language using statistical dynamic time warping for time warping and a separate classifier on the warped features. Suk et al. [20] recognized hand gestures in a continuous video stream by a dynamic Bayesian network. Lamar et al. [21] proposed a neural network, Temporal-CombNET (T-CombNET), and applied it to Japanese-Kana finger spelling recognition. Jerde et al. [22] measured the angles of hand joints for recognizing finger spelling hand shapes, and

- *Y. Jiang is with the Research Institute, Kochi University of Technology, Kami, Kochi 782-8502, Japan. E-mail: jiang.yinlai@kochi-tech.ac.jp.*
- *I. Hayashi is with the Faculty of Informatics, Kansai University, Takatsuki, Osaka 569-1095, Japan. E-mail: ihaya@cbii.kutc.kansai-u.ac.jp.*
- *S. Wang is with the School of Systems Engineering, Kochi University of Technology, Kami, Kochi 782-8502, Japan. E-mail: wang.shuoyu@kochi-tech.ac.jp.*

Manuscript received 21 Jan. 2013; revised 20 Jan. 2014; accepted 12 Mar. 2014. Date of publication 9 Apr. 2014; date of current version 29 Oct. 2014. Recommended for acceptance by L. Khan.
For information on obtaining reprints of this article, please send e-mail to: reprints@ieee.org, and reference the Digital Object Identifier below.
Digital Object Identifier no. 10.1109/TKDE.2014.2316521

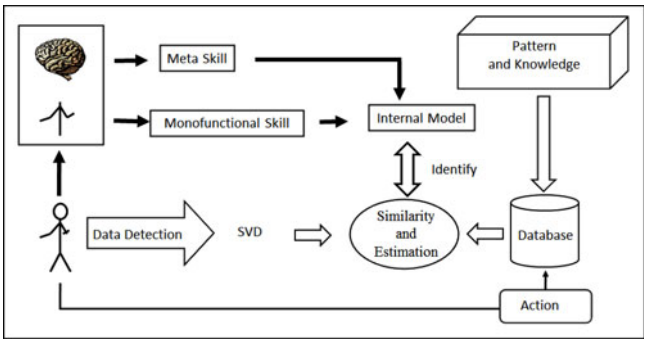

Fig. 1. Conceptual framework of the proposed model.

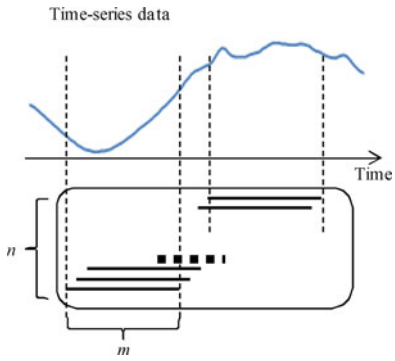

Fig. 2. Design of matrix $M_X^{i,G}$.

reduced the dimensions of the hand by discriminant analysis by Principal Component Analysis (PCA). Gait analysis is also a well studied topic. Daffertshofer et al. [23] suggested the effectiveness of PCA for reducing high-dimensional time-series data sets to a small number of modes in the analysis of gait kinematics. Williamson and Andrews [24] measured the acceleration of the shank and detected the main phases of a normal gait during walking by machine learning. Jakobsen et al. [25] assessed the knee joint range of motion during rehabilitation based on correlation coefficients and the smallest real difference. However, the HMM is not effective when the number of states is large or the data is discontinuous. Since a neural network is too sensitive in time-series data length, the accuracy is not very good. PCA reduces the number of explanatory variables and is a model for visualization with principal component variables. It is possible, however, to lose significant principal component variables when the proportion of variance is low and the number of data is inadequate. In other words, the accuracy of PCA declines when the contribution ratio is low due to a shortage of data.

In this paper, we propose a new method to extract embodied knowledge of body motion by using Singular Value Decomposition (SVD) [26], [27]. Recently, SVD has been used in time-series data analyses for data mining [29] and motion analyses to study the coordinative structures in human behavior [30]. In our method, the left and right singular vectors and the singular values are decomposed from a Hankel matrix defined from the time-series data, which are measured with sensors [28]. Since the left singular vector represents the characteristics of the Hankel matrix and the singular value represents the strength of the corresponding left singular vector, SVD is used more generally as a method for extracting characteristics from observed time-series data.

We applied the proposed method to a hand gesture recognition experiment and a walking disability evaluation experiment. In the hand gesture recognition experiment, we distinguish five kinds of gestures according to the similarity and the estimation by using the left singular vectors. In the walking disability evaluation experiment, we distinguished the levels of walking disability by a three-dimensional hyperplane constructed by singular values. The results of the two experiments suggest that SVD is effective for extracting embodied knowledge from the time-series data. The characteristic and significance of the embodied knowledge extraction using SVD is discussed based on the results of the two experiments.

2 Embodied Knowledge Extraction Using SVD

Suppose M is an m-by-n matrix, then a factorization of M is $M = U\Sigma V$, where $U = (u_1, u_2, \ldots, u_m)$ contains the left singular vectors of M, $V = (v_1, v_2, \ldots, v_n)$ contains the right singular vectors of M, and the matrix Σ is an m-by-n diagonal matrix with nonnegative real singular values on the diagonal. The SVD is an important factorization of a rectangular real or complex matrix with many applications in signal processing and statistics. Applications using SVD include computing the pseudo inverse, least squares data fitting, matrix approximation, and determining the rank, range, and null space of a matrix [26], [27].

Suppose that we measure w points $(P_1, P_2, \ldots, P_w)$ of the body while a person is performing a motion. On point P_i, the measured data series of motion G is denoted as $\tau^{i,G}$. The data series of $\tau^{i,G}$ consists of three-dimensional data $(X^{i,G}, Y^{i,G}, Z^{i,G})$. From this time-series data $\tau^{i,G} = (X^{i,G}, Y^{i,G}, Z^{i,G})$, n vectors by m data sampling are extracted by overlapping and the matrices $M_X^{i,G}$, $M_Y^{i,G}$, and $M_Z^{i,G}$ are constructed as a collective of the measurement data on the X, Y, and Z coordinates of the motion, respectively. Fig. 2 shows a design for constructing the matrix $M_X^{i,G}$. The matrices $M_X^{i,G}$, $M_Y^{i,G}$, and $M_Z^{i,G}$ are described as follows:

$$M_X^{i,G} = \left(X_1^{i,G}, X_2^{i,G}, \ldots, X_n^{i,G}\right)^T \quad (1)$$

$$M_Y^{i,G} = \left(Y_1^{i,G}, Y_2^{i,G}, \ldots, Y_n^{i,G}\right)^T \quad (2)$$

$$M_Z^{i,G} = \left(Z_1^{i,G}, Z_2^{i,G}, \ldots, Z_n^{i,G}\right)^T, \quad (3)$$

where $X_p^{i,G} = (x_{p,1}^{i,G}, x_{p,2}^{i,G}, \ldots, x_{p,m}^{i,G})$, $p = 1, 2, \ldots, n$, and x is a datum on the X coordinate. We define $Y_p^{i,G}$ and $Z_p^{i,G}$ in the same way. Since the matrix is designed by overlapping the extracted data from the whole time-series data, the method using SVD is less constrained by the length of the whole data than those using a neural network. The difference between PCA and our method is that PCA generally analyzes the matrix composed of the deviation of each datum from the empirical mean and does not allow overlap of the measurement data.

Suppose $M_k^{i,G}$, $k = \{X, Y, Z\}$ is an m-by-n matrix as the general format of $M_X^{i,G}, M_Y^{i,G}, M_Z^{i,G}$. The SVD of the matrix $M_k^{i,G}$ is

$$M_k^{i,G} = U_k^{i,G} \Sigma_k^{i,G} \{V_k^{i,G}\}^T, \tag{4}$$

where $U_k^{i,G} = (u_{1,k}^{i,G}, u_{2,k}^{i,G}, \ldots, u_{m,k}^{i,G})$ is an m-by-m unitary matrix, $\{V_k^{i,G}\}^T$ denotes the conjugate transpose of $V_k^{i,G} = (v_{1,k}^{i,G}, v_{2,k}^{i,G}, \ldots, v_{n,k}^{i,G})$ which is an n-by-n unitary matrix, and the matrix $\Sigma_k^{i,G}$ is an m-by-n diagonal matrix. The diagonal entries of $\Sigma_k^{i,G}$ are the singular values of $M_k^{i,G}$. The matrix $U_k^{i,G}$ contains the left singular vectors of $M_k^{i,G}$ and the matrix $V_k^{i,G}$ contains the right singular vectors of $M_k^{i,G}$.

Now, take $M_X^{i,G}$ as an example of matrix $M_k^{i,G}$ to discuss motion analysis. SVD can decompose the matrix $M_X^{i,G}$ into a product of $U_X^{i,G}$, $\Sigma_X^{i,G}$, and $V_X^{i,G}$. Intuitively, the left singular vectors in $U_X^{i,G}$ form a set of patterns of $M_X^{i,G}$ and the diagonal values in matrix $\Sigma_X^{i,G}$ are the singular values, which can be considered as scalars, by which each corresponding left singular vectors affect the matrix $M_X^{i,G}$. Suppose that the number of left singular vectors is l, and the element number of the jth left singular vector is q. Let us denote the couples of the singular values and the left singular vector as $((\sigma_{1,X}^{i,G}, u_{1,X}^{i,G}), (\sigma_{2,X}^{i,G}, u_{2,X}^{i,G}), \ldots, (\sigma_{l,X}^{i,G}, u_{l,X}^{i,G}))$ for $u_{j,X}^{i,G} = (\hat{u}_{1j,X}^{i,G}, \hat{u}_{2j,X}^{i,G}, \ldots, \hat{u}_{hj,X}^{i,G}, \ldots, \hat{u}_{qj,X}^{i,G})$ in the descending order of the singular values, where $\hat{u}_{hj,X}^{i,G}$ is the hth element of the jth left singular vector $u_{j,X}^{i,G}$. The left singular vector expresses the characteristic of the whole time-series data better if its corresponding singular value singular is larger. That is, the greater the singular value is, the more dominant the corresponding pattern is.

3 Gesture Recognition with Left Singular Vectors

The left singular vectors $(u_{1,X}^{i,G}, u_{2,X}^{i,G}, \ldots, u_{l,X}^{i,G})$ well represent the characteristics of motions. We conducted a gesture recognition experiment to demonstrate the effectiveness of feature extraction using the left singular vectors.

3.1 Hand Gesture Measurement

Five kinds of hand gestures, Come here (CH), Go away (GA), Go right (GR), Go left (GL), and Calm down (CD), were performed by two subjects, SW and ST, who were males in their 20s. These gestures are commonly used in daily life. The gestures were performed in a $50\,\mathrm{cm} \times 50\,\mathrm{cm} \times 50\,\mathrm{cm}$ cubic space, whose zero point and coordinate system are shown in Fig. 3. The motions of the hand gestures were measured with Movetr/3D and GE60/W (Library, Tokyo, Japan).The subjects were instructed to finish the gestures within the same speed period since we focused on the trajectory, not the speed of motion. Five markers were measured: P_1 on the tip of the thumb, P_2 on the tip of the middle finger, P_3 on the tip of the little finger, P_4 on the thumb side of the wrist and P_5 on the little finger side of the wrist.

The motions of subject SW are shown in Fig. 4 by nine frames extracted from the experimental video every $1/6$ s.

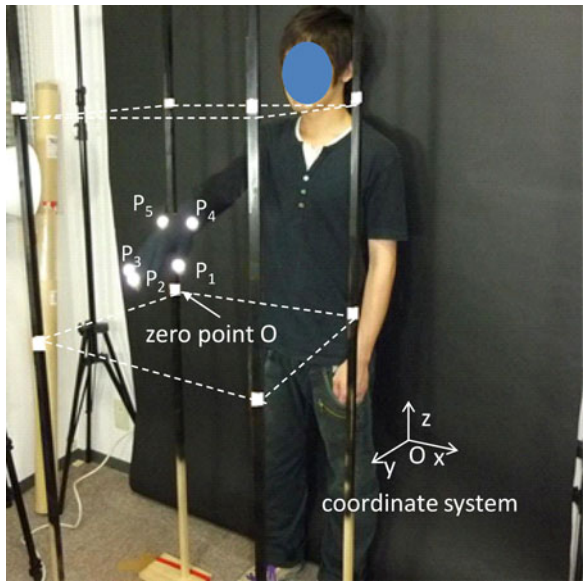

Fig. 3. Environment for measurement of gestures.

The time-series data of P_2 when subject SW performed the five kinds of gestures are shown in Fig. 5. In Fig. 5, the movement change for GA, CH, and CD is large in the top and bottom direction (onto the z-axis) and in the front and back direction (onto the y-axis), and for GR and GL, the movement change is big in the right and left direction (onto the x-axis). One gesture was executed nine times by each subject to get a sufficient variety of motion. The difference between subjects was not the main subject of this study since the restriction of the cubic space eliminates some individual differences. Data of the first five executions were used as the acquisition of patterns of the gesture. Data of the last four times were used to distinguish the gesture.

We proposed two kinds of gesture recognition methods using the left singular vectors extracted from the time-series data of gesture motion: gesture recognition based on the similarity between gesture distances (SGD) and gesture recognition based on the similarity between gesture vectors (SGV). Our aim is to discuss a method to extract embodied knowledge from the time-series data rather than to develop a method to recognize hand gestures.

3.2 Gesture Recognition Based on SGD

Suppose that the observed data series are divided into two groups: $\tau_{TRD}^{i,G}$ as the training data series, and $\tau_{CHD}^{i,G}$ as the checking data series. Let us denote the left singular vector $\tau_{X,TRD}^{i,G}$ for training data related to the X coordinate values of the point P_i on the hand for the gesture G as $U_{X,TRD}^{i,G} = (u_{1,X,TRD}^{i,G}, u_{2,X,TRD}^{i,G}, \ldots, u_{l,X,TRD}^{i,G})$ for $u_{j,X,TRD}^{i,G} = (\hat{u}_{1j,X,TRD}^{i,G}, \hat{u}_{2j,X,TRD}^{i,G}, \ldots, \hat{u}_{hj,X,TRD}^{i,G}, \ldots, \hat{u}_{qj,X,TRD}^{i,G})$. We define the left singular vectors $\tau_{X,CHD}^{i}$ for checking data as $U_{X,CHD}^{i} = (u_{1,X,CHD}^{i}, u_{2,X,CHD}^{i}, \ldots, u_{l,X,CHD}^{i})$, for $u_{j,X,CHD}^{i} = (\hat{u}_{1j,X,CHD}^{i}, \hat{u}_{2j,X,CHD}^{i}, \ldots, \hat{u}_{hj,X,CHD}^{i}, \ldots, \hat{u}_{qj,X,CHD}^{i})$ in the same way.

To recognize the hand gestures, three kinds of similarity criteria are defined on the data $\tau^{i,G} = (X^{i,G}, Y^{i,G}, Z^{i,G})$ as follows:

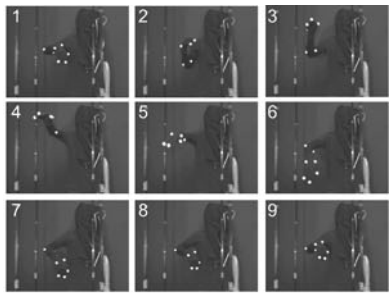

(a) Come Here

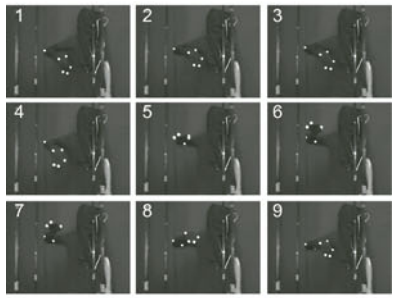

(b) Go Away

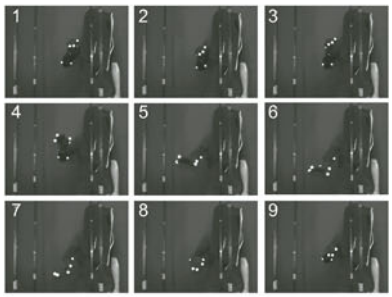

(c) Calm Down

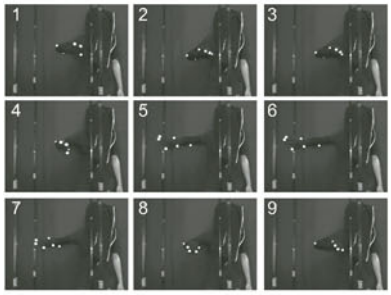

(d) Go Right

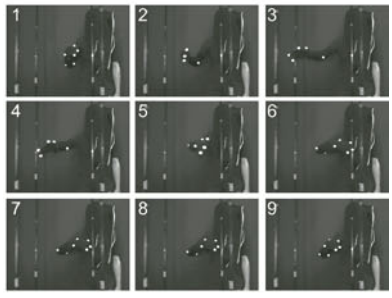

(e) Go Left

Fig. 4. Motion of gestures(representative frames are extracted every 1/6 second).

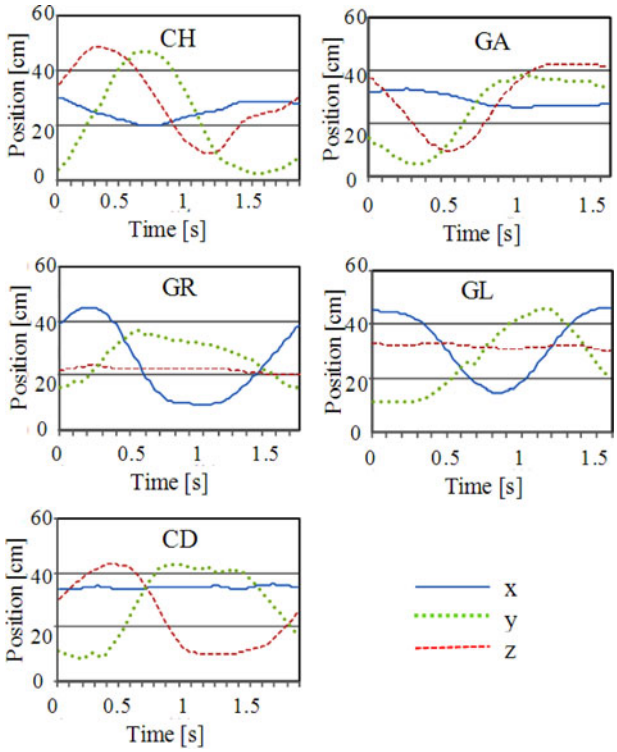

Fig. 5. Time-series data of the gestures(P_2).

$$S_1 : r_i\left(U^{i,G}_{TRD}, U^{i}_{CHD}\right) = \frac{1}{3lq}\sum_{k=1}^{3}\sum_{j=1}^{l}\left|\sum_{h=1}^{q}\hat{u}^{i,G}_{hj,k,TRD} - \sum_{h=1}^{q}\hat{u}^{i}_{hj,k,CHD}\right| \tag{5}$$

$$S_2 : r_i\left(U^{i,G}_{TRD}, U^{i}_{CHD}\right) = \frac{1}{3lq}\sum_{k=1}^{3}\sum_{j=1}^{l}\sum_{h=1}^{q}\left|\hat{u}^{i,G}_{hj,k,TRD} - \hat{u}^{i}_{hj,k,CHD}\right| \tag{6}$$

$$S_3 : r_i\left(U^{i,G}_{TRD}, U^{i}_{CHD}\right) = \frac{1}{3lq}\sum_{k=1}^{3}\sqrt{\sum_{j=1}^{l}\sum_{h=1}^{q}\left(\hat{u}^{i,G}_{hj,k,TRD} - \hat{u}^{i}_{hj,k,CHD}\right)^2}. \tag{7}$$

The similarity S_1 is defined by the absolute differential of the total left singular vector between the training data and the checking data. The similarity S_2 is defined by the total absolute differential of the left singular vectors between the training data and the checking data at the same order. The similarity S_3 is defined by the euclidean distance between the left singular vectors of the training data and the checking data on the multidimensional space.

Since there are w measurement points $(P_1, P_2, \ldots, P_w)$, the estimated gesture G^* is identified by the following two kinds of estimations:

$$E_1 : G^* = \left\{ G_f \middle| \max_f \sum_{i=1}^{w} n\left(G^i_f\right), \quad for \;\; G^i_f = \left\{ G_f \middle| \min_f r_i\left(U^{i,G_f}_{TRD}, U^{i}_{CHD}\right) \right\} \right\} \tag{8}$$

TABLE 1
Gesture Recognition Accuracy Results (SGD)

	Similarity (S_1)	Similarity (S_2)	Similarity (S_3)
Estimation (E_1)	70.0	90.0	80.0
Estimation (E_2)	60.0	80.0	80.0

$$E_2 : G^* = \left\{ G_f | \min_f \sum_{i=1}^{w} r_i\left(U_{TRD}^{i,G_f}, U_{CHD}^{i}\right) \right\}, \quad (9)$$

where G_f is the fth gesture among the five hand gestures, and $n(G_f^i)$ is a counting function, which is $n(G_f^i) = 1$ if the condition G_f^i is satisfied at the P_i point on the hand.

The estimation E_1 is defined by counting the number of minimal similarity values on all the markers and the most counted gesture is output as the recognition result. The estimation E_2 outputs the gesture with the minimal total similarity values as the recognition result.

Table 1 shows the recognition results of the gesture patterns of two subjects based on the three kinds of different similarities, Equations (5), (6), and (7). In the calculation, $m = 125, n = 5, q = 125, l = 1, w = 5$. The recognition results suggest that similarities S_2 and S_3 lead to relatively higher correct recognition rates. Especially, the pair of the similarity S_2 and the estimation E_1 leads to a significantly high accuracy of 90.0 percent. The result suggests that the pair of S_2 and E_1 is more feasible for gesture recognition. However, in general it is hard to distinguish between the gesture of Go Right and Go Left, and so the results are understandable.

In the experiment, the positions of the five markers on the right hand were measured. However, it is possible that not all the positions of these markers have a high relevance to the gestures. We compared the accuracy of each marker for gesture recognition with similarity S_2 and estimation E_1 by calculating the left singular vectors at each marker. Table 2 shows the large counting number of minimized similarity values. The results are shown in the form of a/b, where a is the number of counted times of the most counted gesture and b is the name of the gesture. As a result, the first marker P_1 was selected as the most important marker because the accuracy is the highest, 93.85 percent. Since P_1 measures the time series at the tip of the thumb and is largely related to movement of the thumb, it is suggested that the motion of the thumb is important in gesture recognition. Reducing the number of markers considered in the recognition not only reduces the calculation but also improves the recognition accuracy.

3.3 Gesture Recognition Based on SGV

In the second method, gesture recognition is based on SGV. Now, consider the data series in $M_X^{i,G}$ of Equation (1). If one of the data series $X_p^{i,G}$ is replaced by another data series X_{CHD}^i, the singular values and the left singular vectors of $M_{X,CHD}^i$ are different from those of $M_X^{i,G}$.

$$M_{X,CHD}^i = \left(X_1^{i,G}, \ldots, X_{p-1}^{i,G}, X_{CHD}^i, X_{p+1}^{i,G}, \cdots, X_n^{i,G}\right)^T. \quad (10)$$

TABLE 2
Recognition Accuracy Comparison of Markers (SGD)

Sub./Ges.	Marker				
TW	P_1	P_2	P_3	P_4	P_5
CH	4/GA	4/GA	4/CD	4/GA	4/GA
GA	8/GA	9/GA	9/GA	8/GA	8/GA
GR	7/GR	8/GR	8/GR	6/GR	5/GR
GL	5/GL	4/GL	4/GL	5/GL	5/GL
CD	6/CD	5/GA	5/GA	7/CD	8/CD
ST	P_1	P_2	P_3	P_4	P_5
CH	8/CH	9/CH	11/CH	9/CH	7/CH
GA	7/GA	9/GA	9/GA	9/GA	5/CD
GR	9/GR	10/GR	11/GR	6/GR	9/GR
GL	7/GL	8/GL	10/GL	5/GL	8/GL
CD	4/CD	5/GL	5/GL	5/CD	6/CD
Accuracy (%)	93.85	80.28	81.58	93.75	86.15

The difference between the left singular vectors of $M_X^{i,G}$ and $M_{X,CHD}^i$ is determined by how X_{CHD}^i is different from the other $p-1$ data series. The patterns of $M_{X,CHD}^i$ change more when $X_p^{i,G}$ is replaced by a quite dissimilar data series than when it is replaced by a similar one. Therefore, the difference between the left singular vectors of $M_X^{i,G}$ and X_{CHD}^i can be considered as a measure of the difference between X_{CHD}^i and the other data series. If X_{CHD}^i comes from another kind of hand gesture, the difference can be used as a criterion for judging whether X_{CHD}^i comes from the same kind of hand gesture as the other data series. In our algorithm, the location of X_{CHD}^i is fixed at the end of the data series. Therefore, only the n th $X_n^{i,G}$ is replaced by another data series X_{CHD}^i in Equation (10).

To recognize a hand gesture, three kinds of similarity criteria are defined on the data $\tau^{i,G} = (X^{i,G}, Y^{i,G}, Z^{i,G})$ as follows:

$$S_4 : r_i\left(U_{TRD}^{i,G}, U_{CHD}^{i}\right) = \frac{1}{3lq} \sum_{k=1}^{3} \sum_{j=1}^{l} \left| \sum_{h=1}^{q} \hat{u}_{hj,k,TRD}^{i,G} - \sum_{h=1}^{q} \hat{u}_{hj,k,CHD}^{i} \right| \quad (11)$$

$$S_5 : r_i\left(U_{TRD}^{i,G}, U_{CHD}^{i}\right) = \frac{1}{3lq} \sum_{k=1}^{3} \sum_{j=1}^{l} \sum_{h=1}^{q} \left| \hat{u}_{hj,k,TRD}^{i,G} - \hat{u}_{hj,k,CHD}^{i} \right| \quad (12)$$

$$S_6 : r_i\left(U_{TRD}^{i,G}, U_{CHD}^{i}\right) = \frac{1}{3lq} \sum_{k=1}^{3} \sqrt{\sum_{j=1}^{l} \sum_{h=1}^{q} \left(\hat{u}_{hj,k,TRD}^{i,G} - \hat{u}_{hj,k,CHD}^{i}\right)^2}. \quad (13)$$

The meanings of S_4, S_5, and S_6 are the same as those of S_1, S_2, and S_3, respectively. Since there are w measurement points $(P_1, P_2, \ldots, P_w)$, the estimated gesture G^* is identified by the following estimations:

$$E_3 : G^* = \left\{ G_f | \min_f \sum_{i=1}^{w} r_i\left(U_{TRD}^{i,G_f}, U_{CHD}^{i}\right) \right\}. \quad (14)$$

TABLE 3
Gesture Recognition Accuracy Results (SGV)

Sub.	Ges.	Similarity (S_4)	Similarity (S_5)	Similarity (S_6)
TW	CH	1	2	1
	GA	3	4	4
	GR	2	3	3
	GL	1	3	3
	CD	0	3	3
ST	CH	2	2	2
	GA	1	4	4
	GR	3	4	4
	GL	0	3	2
	CD	0	4	4
Accuracy (%)		30.3	80.0	75.0

TABLE 4
Recognition Accuracy Comparison of Markers (SGV)

Sub./Ges.	Marker				
TW	P_1	P_2	P_3	P_4	P_5
CH	2/GA	2/GA	2/GA	3/GA	2/GA
GA	4/GA	4/GA	2/GA	4/GA	4/GA
GR	3/GR	3/GR	3/GR	3/GR	3/GR
GL	3/GL	3/GL	3/GL	3/GL	3/GL
CD	3/CD	2/GA	3/GA	2/CD	2/CD
ST	P_1	P_2	P_3	P_4	P_5
CH	2/CH	2/CH	2/CH	2/CH	2/CH
GA	4/GA	4/GA	4/GA	4/GA	4/CD
GR	4/GR	4/GR	4/GR	3/GR	3/GL
GL	4/GL	4/GL	4/GL	3/GR	4/GR
CD	4/CD	4/CD	4/CD	3/CD	4/CD
Accuracy (%)	93.94	87.50	83.87	80.00	58.06

In the proposed method, all of the time series must have the same number of data to compose matrix $M_X^{i,G}$, as shown in Equation (1). However, the lengths of the hand gestures in real measurements are different according to the kinds of gestures and the subjects who perform them. Therefore, preprocessing is necessary to make the data series have the same number of data. In this paper, the number of data was set to be the average number. If a data series contains more data than the average number, data are deleted from the data series at the same interval. If a data series contains fewer data than the average number, data are interpolated in the data series at the same interval. The interpolated data are calculated using quadric interpolation.

Table 3 shows the recognition results based on the three kinds of similarity definitions of S_4, S_5, and S_6, in Equations (11), (12), and (13), respectively. The recognition results suggest that the similarity definitions of S_5 and S_6 lead to relatively higher correct recognition rates, but the correct rate of recognition based on S_4 was very low. Therefore, S_5 and S_6 are more feasible in gesture recognition.

As in the comparison of markers in the method by SGD, we compared the accuracy of markers in this method by SGV with similarity S_5 and estimation E_3. Table 4 shows the large counting number of minimized similarity values. The first M_1 was selected as the most important marker, as in Table 2. We realize that the movement of the thumb is most related to gesture recognition by the results. The recognition results of the two methods show that the left singular vectors extracted from the time-series data can be used as knowledge to distinguish gestures. Especially, the total absolute differential of the left singular vectors at the same order is significantly effective because the left singular vectors express a time-dependent weight for identifying the whole movement. Regarding the incorrect recognitions, the motion data were quite similar, although the motion was incorrectly recognized as a gesture different from the intended one. Gestures GR and GL, for example, have opposite meanings but their motions are very similar in that the hand waves left and right. Their difference between the two gestures is the hand moves faster from left to right in GR while it moves faster from the right to left in GL. Even human beings sometimes do not distinguish correctly between them [31]. On the other hand, the differences between subjects were not considered in the experiment due to the restrictions of the measurement environment. Further study will discuss individual differences by carrying out experiments with more subjects.

We compared our motion analysis method using SVD with the following traditional methods: a PCA clustering method, a PCA distance method, and a correlation efficiency (CE) method. We used the gesture distance method that distinguishes gesture movements with similarity S_2 and estimation E_1, and the gesture vector method that distinguishes gesture movements with similarity S_5 and estimation E_3. For the correlation coefficient method, the combination of similarity S_7 and estimation E_4 is adopted to calculate the recognition accuracy. The following combination of similarity S_8 and estimation E_5 is adopted for the PCA clustering method, and the combination of similarity S_9 and estimation E_5 is adopted for the PCA distance method.

$$S_7 : r_i\left(U_{TRD}^{i,G}, U_{CHD}^{i}\right) = \frac{1}{3}\sum_{k=1}^{3} R\left(d_{TRD,k}^{i,G}, d_{CHD,k}^{i}\right) \tag{15}$$

$$S_8 : r_i\left(U_{TRD}^{i,G}, U_{CHD}^{i}\right) = \min_f \sqrt{\sum_{c=1}^{H}\left(f_{XYZ\to c}\left(E\left(d_{TRD}^{i,G_f}\right)\right) - f_{XYZ\to c}\left(E\left(d_{CHD}^{i}\right)\right)\right)^2} \tag{16}$$

$$S_9 : r_i\left(U_{TRD}^{i,G}, U_{CHD}^{i}\right) = \min_f \sqrt{\sum_{c=1}^{H}\left(f_{G_f\to c}\left(d_{TRD}^{i,G_f}\right) - f_{G_f\to c}\left(d_{CHD}^{i}\right)\right)^2} \tag{17}$$

$$E_4 : G^* = \left\{ G_f \middle| \max_f \frac{1}{w}\sum_{i=1}^{w} r_i\left(U_{TRD}^{i,G_f}, U_{CHD}^{i}\right) \right\} \tag{18}$$

TABLE 5
Recognition Accuracy of Methods

Marker	Ges. Dist.	Ges. Vec.	Corre. Co.	PCA Clus.	PCA Dist.
P_1	93.85	93.94	60.0	20.0	60.0
P_2	80.28	87.5	80.0	40.0	80.0
P_3	81.58	83.87	80.0	60.0	40.0
P_4	93.75	80.0	80.0	40.0	40.0
P_5	86.15	58.06	60.0	20.0	40.0
Average	87.12	80.67	72.0	36.0	52.0
All Markers	90.0	80.0	70.0	60.0	40.0

$$E_5 : G^* = \left\{ G_f | \max_f \sum_{i=1}^{w} n\big(r_i(U_{TRD}^{i,G_f}, U_{CHD}^{i})\big) \right\}, \qquad (19)$$

where $R(x, y)$ is the correlation coefficient between x and y. $E(\,)$ is an average, $f_{A\to B}(\,)$ is a function of the PCA, which converts from the variable A to the principal axis B, and H is the number of principal axes, where we set $H = 3$.

The results are shown in Table 5. The average accuracy of the two methods we proposed, which are the method based on SGD and the method based on SGV, are much higher with values of 90.0 and 80.0 percent when considering all the markers, and with average values of 87.12 and 80.67 percent when considering each marker separately. None of the other three methods obtained an accuracy higher than 80.0 percent, regardless of whether all the markers were considered or each marker was considered separately. The reason for the low accuracy is that PCA and CE depend strongly on the length of the data. The difference between the lengths of the TRD for training and the CHD for checking leads to the low recognition accuracy. In contrast, since our methods using SVD can extract a movement characteristic regardless of the length of the time-series data, they do not depend on the data length because of the overlapping of subsets of the time-series data, which contributes to the high recognition accuracy.

3.4 Knowledge Representation with Fuzzy If-Then Rules

The results of Sections 3.2 and 3.3 illustrate that the features of gesture motion are extracted into the left singular vectors. The features can be used to classify the gestures with a high degree of accuracy by using a proper calculation. In order to understand the features better, an intuitive and understandable way to represent these features are required. In this section, the features of the left singular vectors are described as fuzzy sets, and fuzzy if-then rules [32] are used to represent the knowledge.

The frequency distribution of the elements in the left singular vectors is shown by histograms. The histograms of the 1st–3rd left singular vectors are shown in Fig. 6 as examples. The singular vectors were calculated from $M_X^{1,GA}$, that is, the matrix composed from the x coordinate time-series data at point 1 of gesture GA. The elements are between -0.4 and 0.4, and are counted in four intervals: $(-0.4, 0.2)$, $[0.2, 0)$, $[0, 0.2)$, and $[0.2, 0.4)$.

The features of the histograms can be described by quadrilateral fuzzy sets. A quadrilateral fuzzy set is denoted as $Q(a_1(d_1), a_2(d_2), a_3(d_3), a_4(d_4))$, where $a_1 \sim a_4$ are the lateral coordinates, and $d_1 - d_4$ the vertical

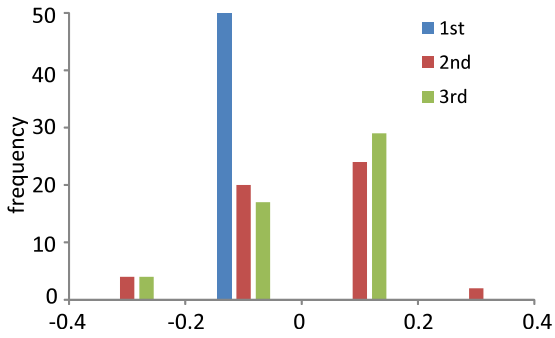

Fig. 6. Element histogram of the 1st–3rd left singular vectors (P_1 of GA).

coordinates of the vertices of the quadrilateral. $d_1 \sim d_4$ are the grade of membership of $a_1 \sim a_4$. $a_1 \sim a_4$ and $d_1 \sim d_4$ are determined to make the quadrilateral fuzzy set to approximate the shape of the histogram with d_1 and d_4 being 0, the maximum of d_2 and d_3 being 1, a_2 and a_3 being -0.1 and 0.1 respectively. Fig. 7 shows the quadrilateral fuzzy sets of the corresponding histograms in Fig. 6. The fuzzy sets for the 1st-3rd left singular vectors are $Q(-0.3(0), -0.1(1), 0.1(0), 0.3(0))$, $Q(-0.35(0), -0.1(0.83), 0.1(1), 0.32(0))$, and $Q(-0.35(0), -0.1(0.59), 0.1(1), 0.3(0))$, respectively.

After describing the features of the left singular vectors as fuzzy sets, the fuzzy if-then rule to represent the knowledge assumes the following form

$$if \bigwedge_{i=1}^{w} \bigwedge_{k=1}^{3} \bigwedge_{j=1}^{l} \left(Q_{l,k}^{i,G^*} \;\; is \;\; Q_{l,k}^{i,G}\right) \quad then \;\; G^* \;\; is \;\; G, \qquad (20)$$

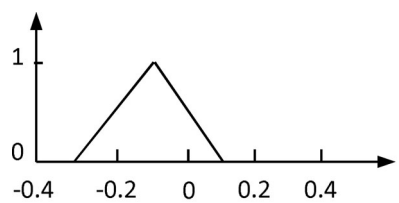

(a) 1st

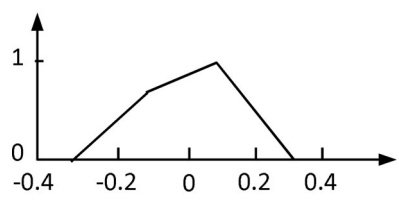

(b) 2nd

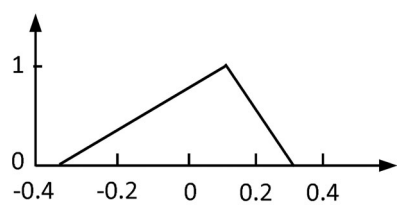

(c) 3rd

Fig. 7. Membership functions of the 1st-3rd left singular vectors (P_1 of GA).

Fig. 8. Experimental settings for ambulation.

where Q is a quadrilateral fuzzy set to represent the jth singular vector on the kth coordinate at the ith marker. Since these fuzzy rules represent the knowledge about the features of the gestures, gesture recognition can be realized by fuzzy reasoning based on these rules.

4 Walking Disability Evaluation Using Singular Values

Accelerometers have been widely used to monitor body movements, including gait, sit-to-stand transfers, postural sway, and falls, for its low cost, less restriction and wearability [33], [34]. In clinician, they have been used to measure physical activity levels and to identify and classify movements performed by subjects [24], [35], to analyze gait pattern in diseases, such as Parkinson disease [36], [37] and stroke [38], [39], and to monitor patient [40]. Since the singular value indicates the strength of the corresponding left singular vector, which represents the characteristics of the Hankel matrix, we used the singular values calculated from the walking acceleration data to evaluate the levels of walking disability.

4.1 Acceleration Measurement with Wearable Wireless Accelerometers

In the experiment, the acceleration during walking was measured by three wearable wireless three-axis accelerometers (Motion Recorder MVP-RF8, Microstone Nagano, Japan): P_1 on the back of the waist (B. Waist), P_2 on the midpoint of the right shank (R. M. Shank), and P_3 on the midpoint of the left shank (L. M. Shank), as shown in Fig. 8. The sampling rate of the sensor was 100 Hz. When the subject stands upright, the sensors' x-axis is front/back, the y-axis is up/down, and the z-axis is right/left. However, the coordination system changes since the orientation of the sensors changes during walking. In the experiment, we examined the acceleration of walking difficulty simulated by restricting the right leg with knee supporters and weight bands

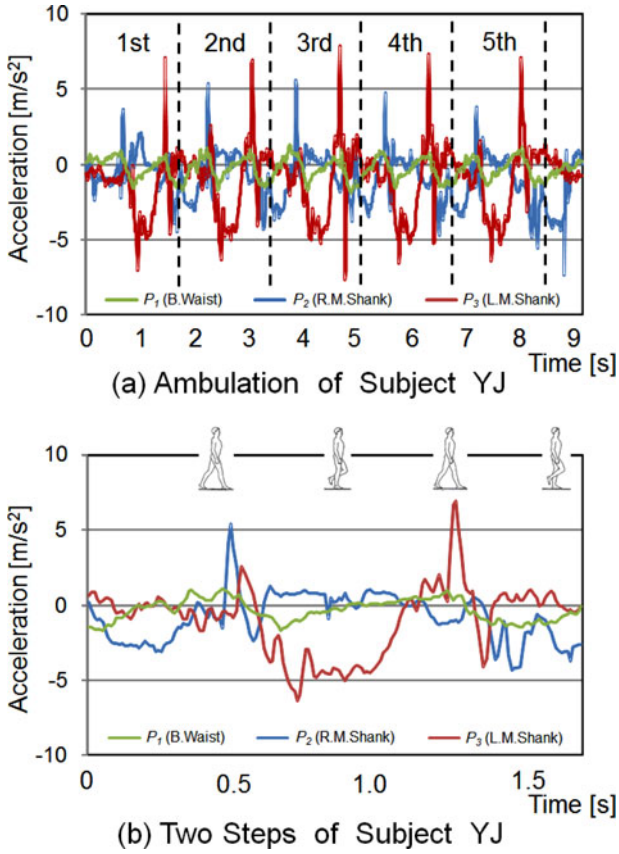

Fig. 9. Example of ambulation.

(Fig. 8). The knee supporter bound around the knee joint decreases the knee joint range of motion and the weight band bound around the ankle joint can simulate the weakness in muscle strength. The simulation is very important in testing our method since it does not endanger the safety of the disabled during the development phase of the method. Two levels of walking difficulty were simulated by two levels of restraint in the experiment. A weak restraint was simulated with one knee supporter and one weight band (1 kg), and a strong restraint with two knee supporters and two weight bands (2 kg). In total, three statuses (Normal without restraint, Weak, and Strong) were examined.

Six healthy volunteers (YJ, TK, KT, KS, TF, and RT; 5 males and 1 female) aged 21–31 yr (mean 26 yr) participated in the experiment. The subjects were instructed to walk for approximately 4 m along a straight line. The experiment was carried out in the status order of Normal, Weak, and Strong. For each status, each subject walked four times.

The measurement time-series data in the x coordinate of the three sensors when subject YJ walked in the status of Weak are shown in Fig. 9. The fluctuation of the acceleration was significant when the right foot or the left foot was landing. Fig. 9a shows five strides. The acceleration data of the first stride were extracted and are shown in Fig. 9b. All the acceleration at the B. Waist, R. M. Shank, and L. M. Shank significantly fluctuated when the right foot pushed off from the floor or stepped on the floor. The fluctuation in the acceleration at L. M. Shank was more significant than that at R. M. Shank

TABLE 6
Singular Values of Ambulation Experiment

Subject	Restraint Ambulation	P_1			P_2			P_3		
		X	Y	Z	X	Y	Z	X	Y	Z
TF	Normal	17.7	23.4	21.8	57.9	52.7	50.9	46.8	55.6	33.4
	Weak	17.0	23.3	26.9	33.3	34.7	39.4	42.5	48.0	28.4
	Strong	17.6	22.8	27.3	31.7	30.3	37.7	40.4	43.1	27.8
YJ	Normal	11.4	9.4	12.1	45.9	40.5	22.2	47.3	48.2	18.9
	Weak	10.9	8.2	15.4	23.4	11.2	13.9	43.9	33.5	14.7
	Strong	18.3	10.4	18.5	19.5	10.2	13.0	42.0	25.6	13.7
TK	Normal	18.1	19.3	12.6	51.1	34.3	34.0	51.9	47.8	30.1
	Weak	20.6	20.4	17.0	27.5	25.1	26.4	45.7	45.8	27.3
	Strong	20.2	20.0	15.7	25.3	20.1	21.9	42.8	38.5	27.7
KS	Normal	20.2	19.0	12.8	60.4	58.8	36.3	57.3	66.4	25.8
	Weak	19.7	15.8	19.0	36.8	32.0	21.5	52.4	55.0	20.1
	Strong	18.8	15.9	19.2	33.5	29.3	18.9	39.6	34.6	19.3
RT	Normal	28.0	24.5	19.6	70.8	53.7	37.5	58.7	58.0	32.5
	Weak	24.5	22.3	17.8	60.7	34.9	27.3	56.9	58.1	30.4
	Strong	22.5	23.7	19.1	51.5	33.3	20.8	50.3	52.7	26.1
KT	Normal	23.4	27.5	17.9	57.1	65.3	40.3	60.6	74.3	32.0
	Weak	21.6	31.5	24.3	40.3	37.4	25.4	46.0	59.6	22.1
	Strong	18.5	24.3	22.4	38.5	26.8	16.0	38.5	46.4	16.4
Ave.	Normal	19.8	20.5	16.1	57.2	50.9	36.9	53.8	58.4	28.8
	Weak	19.1	20.3	20.1	37.0	29.2	25.7	47.9	50.0	23.8
	Strong	19.3	19.5	20.4	33.3	25.0	21.4	42.3	40.2	21.8

since the right leg was restricted by the knee supporter and the weight band. The fluctuation in the acceleration at B. Waist was the smallest among the three measurement points. This showed that the trunk of the body, especially the waist, was kept relatively stable to maintain the body balance even when the lower limbs were disabled.

4.2 Relationship between Singular Values and Walking Disability

We focused on the acceleration change around the time when the right foot pushed off and stepped on the floor. The acceleration data around the right foot landing were analyzed. Matrix M for SVD was designed according to the local maximum turning points, as shown in Fig. 9. It took five strides to walk 4 m in the experiment. The acceleration data of the middle three strides, which do not involve the initiation and termination of the walking movement, were extracted for analysis. The data from 0.5 s before the maximum turning point to 0.5 s after the maximum turning point were extracted as column vectors. For each turning point, nine column vectors (three sensors, each of which has three coordinates) were extracted. The column vectors from the same acceleration data series composed matrix M. Therefore, M was a matrix of 100 rows and three columns. In this paper, only the first singular value and the first left singular vector were considered. Thus parameter l was 1.

The first singular values extracted from the acceleration data with SVD are listed in Table 6. In spite of the individual differences in walking, similar changes of the singular values of all six subjects are shown. The singular values of P_2 and P_3 decreased with the increase of walking difficulty, and especially those of P_2 decreased in all three axes, X, Y, and Z. However, the decrease did not show at P_1. The Waist is the center of the body and is always kept balanced during movement. Fig. 9 shows that the waist was relatively stable to maintain the body balance. An F-test was performed on the singular values at P_2 to assess the significance of the difference among the three levels. The F-test results in Table 7 show that for all three axes, the singular values are significantly different between the three levels. The first singular values of P_2, therefore, are suggested to be an effective criterion to evaluate walking difficulty. That is, the first singular values from the acceleration of the restricted leg decreases with the increase of walking difficulty. The larger the first singular values at P_2 are, the more serious the walking disability is.

TABLE 7
Result of F Test on P_2

	Variation Factor	Sum of Sq.	df	Mean Sq.	F Val.	P Val.
X	Be.Gr.	7902.4	2	3951.2	33.56	6.61E-11
	With.Gr.	8123.9	69	117.7		
	Total	16026.3	71			
Y	Be.Gr.	9263.1	2	4631.5	47.76	9.56E-14
	With.Gr.	6690.9	69	97.0		
	Total	15954.0	71			
Z	Be.Gr.	7902.4	2	1536.8	21.13	6.93E-08
	With.Gr.	8123.9	69	72.7		
	Total	16026.3	71			

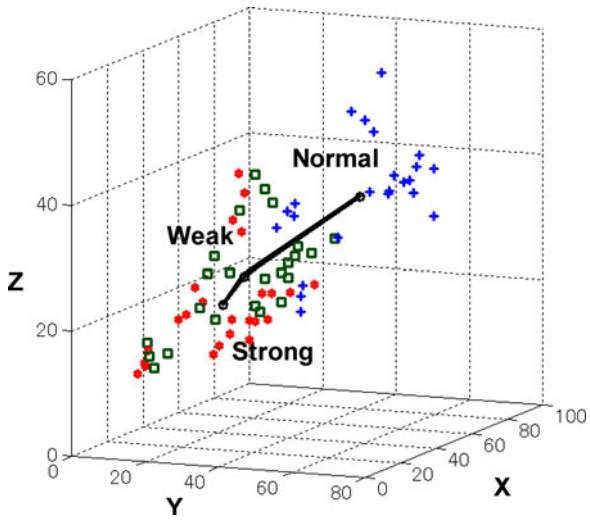

Fig. 10. Singular values of the three statuses.

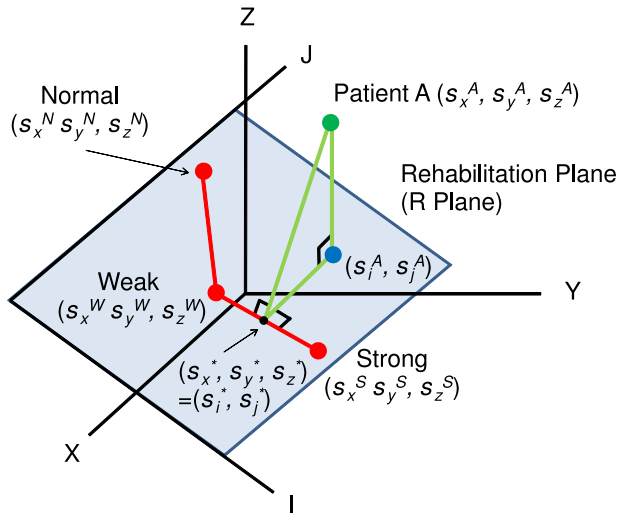

Fig. 11. Conceptual diagram of R-Plane.

4.3 R-Plane for Visualization of Walking Disability

The results in Table 6 suggest that the first singular values can be used as the criterion for the evaluation of walking disability. In practical applications, walking ability assessment is important to track recovery and design a proper rehabilitation program according to the condition of the patient during the process of walking rehabilitation. Clinical measurements of walking ability are mainly based on inspection by the physical therapist, sometimes with the help of muscle strength measurement, X-ray examination, ground reaction force, 3D motion analysis, acceleration analysis, gait and stride analysis, electromyography (EMG), and so on [39]. Objective measurements and correct interpretation of the measurement results can have a substantial impact on the recovery. A convenient assessment method is desired for those who rehabilitate and exercise at home, because they can know their status anytime by themselves.

To provide a more understandable presentation of the data for the physical therapists and the patients to evaluate the recovery of walking ability by using the singular values calculated from the walking acceleration, we propose a visualization tool, called a rehabilitation plane (R-Plane), to assist in the evaluation of walking disability. The first singular values extracted from the acceleration data at P_2 are plotted in 3D space in Fig. 10. The singular values of four times of walking are plotted in a different shape and color according to the status. The average singular values of the three statuses, $(\sigma_x^N, \sigma_y^N, \sigma_z^N)$ for Normal, $(\sigma_x^W, \sigma_y^W, \sigma_z^W)$ for Weak, and $(\sigma_x^S, \sigma_y^S, \sigma_z^S)$ for Strong, are connected by black lines. Fig. 10 shows that the first singular values are clustered according to the status. The line connecting the average values can be considered as the line of severity of walking difficulty. A plane can be defined by the average singular values of the three statuses. Given a patient's singular values of walking, a perpendicular line is drawn from the point defined by the singular values to the lines connecting the average singular values; then, the patient's walking disability can be evaluated intuitively by the position of the intersection point. This plane is called the R-Plane, which can be used for walking disability evaluation in rehabilitation to assess the recovery of patients.

The conceptual diagram of the R-Plane is shown in Fig. 11. Suppose the normal vector of the R-Plane is $\vec{n} = (n_x, n_y, n_z)$, then the R-Plane can be described by Equation (21).

$$n_x\left(x - \sigma_x^N\right) + n_y\left(y - \sigma_y^N\right) + n_z\left(z - \sigma_z^N\right) = 0. \qquad (21)$$

Suppose the coordinate of patient A in 3D space is $(\sigma_X, \sigma_Y, \sigma_Z)$, whose projection to the R-Plane is (σ_i^R, σ_j^R). The projection of (σ_i^R, σ_j^R) to the line connecting the average singular values is $(\sigma_i^*, \sigma_j^*) = (\sigma_X^*, \sigma_Y^*, \sigma_Z^*)$. Then the walking disability and recovery of patient A can be assessed by the position of (σ_i^*, σ_j^*) and the distances of (σ_i^R, σ_j^R) to the average singular values.

As an example, we consider subject TK as patient A and draw the R-Plane based on the average singular values of the other five subjects. The equation of the plane is

$$-0.810x + 0.532y + 0.246z + 9.284 = 0. \qquad (22)$$

The R-Plane is shown in Fig. 12. Subject TK's singular values in the statuses of Normal, Weak, Strong are (NL, WC, SC), whose projection to the lines in the R-Plane are (NL^*, WC^*, SC^*). Although status Normal is not very accurate, statuses Weak and Strong are correctly located in the figure. The results show the effectiveness of the R-Plane in intuitively presenting the walking disability and providing visual information of the patient's recovery.

5 Discussion

A new method for embodied knowledge extraction from the time-series data of motion by using singular value decomposition is proposed and evaluated by a hand gesture recognition experiment and a walking disability assessment experiment. We design a matrix by overlapping the subsets of the time-series data and use the left singular vectors of the matrix as the patterns of the motion and the singular value as a scalar, by which the corresponding left singular vector affects the matrix.

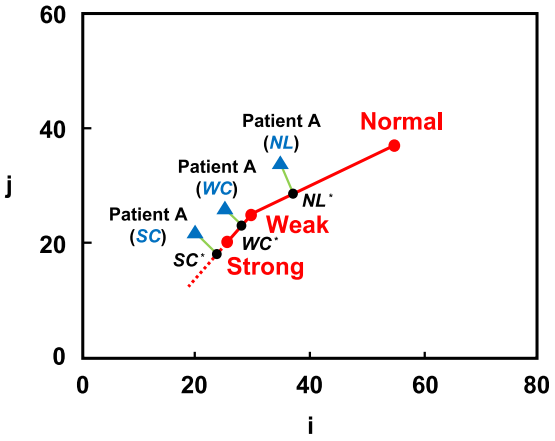

Fig. 12. Example of R-Plane.

Since the method is less affected by the length of the time-series data, it leads to higher accuracy of hand gesture recognition than do conventional methods using PCA or CE. Both the recognition based on SGD and the recognition based on SGV obtained the best accuracy with the same similarity calculation, S_2 and S_5. The similarities S_2 and S_5 are defined by the total absolute differential of the left singular vectors between the training data and the checking data at the same order. It is suggested that the order of the time-series data is an important characteristic of the time-series data and the left singular vector is able to extract that characteristic. As for the estimation methods, E_1, which is defined by counting the number of minimal similarity values on all the markers, obtained better accuracy. Motion analysis usually deals with data from multiple sensors and the sensors are related to each other; for example, P_4 and P_5 in the gesture motion measurement, which are on the thumb side of the wrist and on the little finger side of the wrist, respectively, are highly correlated. In this case, a decision by the majority is more effective than averaging or summing.

The recognition results on each marker show that on P_1, the recognition accuracy is the highest with the value of 93.85 percent. Fig. 13 is a plot of the results in Tables 2 and 3 for the position of the five markers. On average, the markers on the thumb side of the arm obtained higher recognition accuracy. This may be because when a hand gesture is performed, the thumb side of the arm attracts more attention, since it is in the view of the performer, and thus the motion is more consistent.

The first singular values calculated from the walking acceleration were suggested to be effective to evaluate the levels of walking disability. The singular value is considered as a scalar, by which the corresponding left singular vector affects the original matrix. Walking with different disabilities has a similar pattern or characteristic. However, the strength of the most dominant characteristic, which is the first singular vector, is significantly different. The singular values can be utilized as a criterion for the evaluation of recovery in walking rehabilitation. An R-Plane, defined by the singular values from the walking acceleration, is proposed as a visualization tool to assist the evaluation of the walking disability.

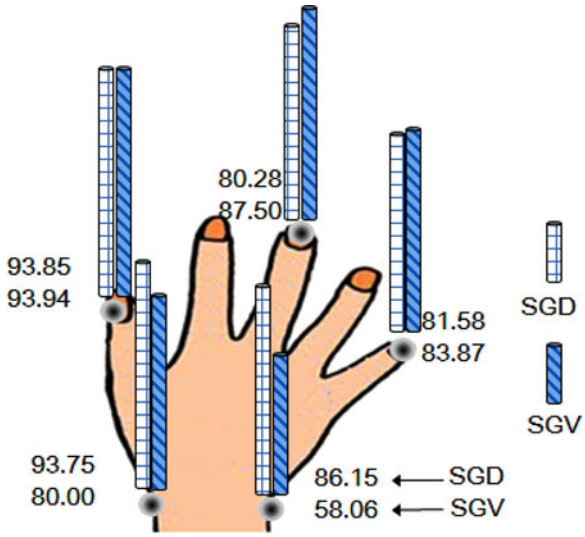

Fig. 13. Recognition result of each marker.

The physical therapist and the patient can intuitively evaluate the recovery progress with the R-Plane.

We propose to extract embodied knowledge by identifying the relationship between the sensor input and the output of the internal model. The mechanism underlying the skillful movement which a human being performs unconsciously is still not sufficiently elucidated from the viewpoints of neurophysiology or the structure of the body. The motion analysis method using SVD we propose is effective to extract embodied knowledge from motion by obtaining the characteristics and their strength. Its effectiveness was validated by the gesture recognition experiment, which measured the position of the measurement points, and the walking disability experiment, which measured the acceleration of the measurement points. Our aim was to discuss the method to extract embodied knowledge from the time-series data rather than to develop methods to recognize hand gestures and to evaluate walking disability, and fairly good results were obtained with the proposed method.

6 Conclusion

A new method for embodied knowledge extraction from the time-series data of motion is proposed by using SVD. We applied the method to a gesture recognition experiment and a walking disability evaluation experiment. The effectiveness of extracting the motion pattern with the left singular vectors in gesture recognition was validated by comparison with conventional methods PCA and CE. In addition, the effectiveness of evaluating the strength of the dominant motion pattern affecting the motion with the singular values was shown by the significantly different first singular values among the three levels of walking difficulty, normal, weak, and strong. Motion analysis using SVD is suggested as a useful method to extract embodied knowledge from motion measurement data.

Acknowledgments

This work was supported by the Strategic Project to Support the Formation of Research Bases at Private Universities:

Matching Fund Subsidy from MEXT (Ministry of Education, Culture, Sports, Science and Technology), 2008-2012, and JSPS KAKENHI Grant Numbers 23240088, 22300197, and 23700316.

REFERENCES

[1] L. E. Holt and S. L. Beilock, "Expertise and its embodiment: Examining the impact of sensorimotor skill expertise on the representation of action-related text," *Psychonomic Bulletin Rev.*, vol. 13, no. 4, pp. 694–701, Aug. 2006.

[2] D. C. Spencer, "Habit(us), body techniques and body callusing: An ethnography of mixed martial arts," *Body Soc.*, vol. 15, no. 4, pp. 119–143, Dec. 2009.

[3] S. Furuya and H. Kinoshita, "Organization of the upper limb movement for piano key-depression differs between expert pianists and novice players," *Exp. Brain Res.*, vol. 185, no. 4, pp. 581–593, Mar. 2008.

[4] S. Furuya, R. Osu, and H. Kinoshita, "Effective utilization of gravity during arm downswing in keystroke by expert pianists," *Neurosci.*, vol. 164, no. 2, pp. 822–831, Dec. 2009.

[5] R. C. Miall, D. J. Weir, D. M. Wolpert, and J. F. Stein, "Is the cerebellum a Smith predictor?" *J. Motor Behavior*, vol. 25, pp. 203–216, Sep. 1993.

[6] R. C. Miall and J. K. Jackson, "Adaptation to visual feedback delays in manual tracking: Evidence against the Smith Predictor model of human visually guided action," *Exp. Brain Res.*, vol. 172, no. 1, pp. 77–84, Jun. 2006.

[7] M. Kawato, "Internal models for motor control and trajectory planning," *Current Opinion Neurobiol.*, vol. 9, no. 6, pp. 718–727, Dec. 1999.

[8] H. Imamizu and M. Kawato, "Cerebellar internal models: Implications for the dexterous use of tools," *Cerebellum*, vol. 11, no. 2, pp. 325–335, Jun. 2012.

[9] J. K. Aggarwal and Q. Cai, "Human motion analysis: A review," *Comput. Vis. Image Understanding*, vol. 73, no. 3, pp. 428–440, Mar. 1999.

[10] J. K. Aggarwal and M. S. Ryoo, "Human activity analysis: A review," *ACM Comput. Surveys*, vol. 43, no. 3, Article 16, p. 43, 2011.

[11] R. Balasubramaniam and M. T. Turvey, "Coordination modes in the multisegmental dynamics of Hula hooping," *Biol. Cybern.*, vol. 90, pp. 176–190, Apr. 2004.

[12] M. Hirashima, K. Kudo, K. Watarai, and T. Ohtsuki, "Control of 3D limb dynamics in unconstrained overarm throws of different speeds performed by skilled baseball players," *J. Neurophysiol.*, vol. 97, no. 1, pp. 680–691, Jan. 2007.

[13] Y. Nakayama, K. Kudo, and T. Ohtsuki, "Variability and fluctuation in running gait cycle of trained runners and non-runners," *Gait Posture*, vol. 31, no. 3, pp. 331–335, Mar. 2010.

[14] K. Furukawa, S. Igarashi, K. Ueno, T. Ozaki, S. Morita, N. Tamagawa, T. Okuyama, and I. Kobayashi., "(2002.) Modeling human skill in Bayesian network," *Linkoping Electronic Articles in Computer and Information Science*, vol. 7, Linkoping Unive. Electron. Press, [Online]. Available: http://www.ida.liu.se/ext/epa/cis/2002/012/tcover.html

[15] K. Furukawa, T. Masuda, and I. Kobayashi, "Abductive reasoning as an integrating framework in skill acquisition," *J. Adv. Comput. Intell. Intell. Informat.*, vol. 15, no. 8, pp. 954–961, Oct. 2011.

[16] S. Mitra and T. Acharya, "Gesture recognition: A survey," *IEEE Trans. Syst., Man, Cybern., Part C*, vol. 37, no. 3, pp. 311–324, May 2007.

[17] A. D. Wilson and A. F. Bobick, "Parametric hidden Markov models for gesture recognition," *IEEE Trans. Pattern Anal. Mach. Intell.*, vol. 21, no. 9, pp. 884–900, Sep. 1999.

[18] T. Pylvanainen, "Accelerometer based gesture recognition using continuous HMMs," in *Proc. 2nd Iberian Conf. Pattern Recognit. Image Anal.*, Jun. 2005, pp. 639–646.

[19] J. F. Lichtenauer, E. A. Hendriks, and M. J. T. Reinders, "Sign language recognition by combining statistical DTW and independent classification," *IEEE Trans. Pattern Anal. Mach. Intell.*, vol. 30, no. 11, pp. 2040–2046, Nov. 2008.

[20] H. I. Suk, B. K. Sin, and S. W. Lee, "Hand gesture recognition based on dynamic Bayesian network framework," *Pattern Recognit.*, vol. 43, no. 9, pp. 3059–3072, Sep. 2010.

[21] M. V. Lamar, M. S. Bhuiyan, and A. Iwata, "Hand gesture recognition using T-CombNET: A new neural network model," *IEICE Trans. Inf. Syst.*, vol. E83-D, no. 11, pp. 1986–1995, Nov. 2000.

[22] T. E. Jerde, J. F. Soechting, and M. Flanders, "Biological constraints simplify the recognition of hand shapes," *IEEE Trans. Biomed. Eng.*, vol. 50, no. 2, pp. 265–269, Feb. 2003.

[23] A. Daffertshofer, C. J. Lamoth, O. G. Meijer, and P. J. Beek, "PCA in studying coordination and variability: A tutorial," *Clinical Biomechanics*, vol. 19, no. 4, pp. 415–428, May 2004.

[24] R. Williamson and B. J. Andrews, "Gait event detection for FES using accelerometers and supervised machine learning," *IEEE Trans. Rehabil. Eng.*, vol. 8, no. 3, pp. 312–319, Sep. 2000.

[25] T. L. Jakobsen, M. Christensen, S. S. Christensen, M. Olsen, and T. Bandholm, "Reliability of knee joint range of motion and circumference measurements after total knee arthroplasty: Does tester experience matter?" *Physiotherapy Res. Int.*, vol. 15, no. 3, pp. 126–134, Sep. 2010.

[26] M. E. Wall, A. Rechtsteiner, and L. M. Rocha, "Singular value decomposition and principal component analysis," in *A Practical Approach to Microarray Data Analysis*, D. P. Berrar, W. Dubitzky, and M. Granzow, eds., Norwell, MA, USA: Kluwer, pp. 91–109.

[27] D. B. Skillicorn, "Understanding Complex Datasets: Data Mining with Matrix Decompositions," Boca Raton, FL, USA, CRC Press, May, 2007.

[28] Y. Jiang, I. Hayashi, M. Hara, and S. Wang, "Three-dimensional motion analysis for gesture recognition using singular value decomposition," in *Proc. IEEE Int. Conf. Inf. Autom.*, Jun. 2010, vol. 15, no. 8, pp. 805–810.

[29] T. Ide and K. Inoue, "Knowledge discovery from heterogeneous dynamic systems using change-point correlations," in *Proc. SIAM Int. Conf. Data Mining*, New Orleans, USA, Jul. 2005, pp. 571–576.

[30] H. Nakanishi, S. Kanata, H. Hattori, T. Sawaragi, and Y. Horiguchi, "Extraction of coordinative structures of motions by segmentation using singular spectrum transformation," *J. Adv. Comput. Intell. Intell. Inf.*, vol. 15, no. 8, pp. 1019–1029, Oct. 2011.

[31] A. Kendon, *Gesture: Visible Action as Utterance*. Cambridge, U.K.: Cambridge Univ. Press, 2004.

[32] L. A. Zadeh, "Toward a theory of fuzzy information granulation and its centrality in human reasoning and fuzzy logic," *Fuzzy Sets Syst.*, vol. 90, no. 2, pp. 111–127, Sep. 1997.

[33] K. M. Culhane, M. O'Connor, D. Lyons, and G. M. Lyons, "Accelerometers in rehabilitation medicine for older adults," *Age Aging*, vol. 34, no. 6, pp. 556–560, Nov. 2005.

[34] J. J. Kavanagh and H. B. Menz, "Accelerometry: A technique for quantifying movement patterns during walking," *Gait Posture*, vol. 28, no. 1, pp. 1–15, Jul. 2008.

[35] H. Lau and K. Tong, "The reliability of using accelerometer and gyroscope for gait event identification on persons with dropped foot," *Gait Posture*, vol. 27, no. 2, pp. 248–257, Feb. 2008.

[36] A. Salarian, H. Russmann, F. J. Vingerhoets, C. Dehollain, Y. Blanc, P. R. Burkhard, and K. Aminian, "Gait assessment in Parkinson's disease: Toward an ambulatory system for long-term monitoring," *IEEE Trans. Biomed. Eng.*, vol. 51, no. 8, pp. 1434–1443, Aug. 2004.

[37] M. Yoneyama, Y. Kurihara, K. Watanabe, and H. Mitoma, "Accelerometry-based gait analysis and its application to parkinson's disease assessment—part 2 : A new measure for quantifying walking behavior," *IEEE Trans. Neural Syst. Rehabil. Eng.*, vol. 21, no. 6, pp. 999–1005, Nov. 2013.

[38] M. Iosa, G. Morone, A. Fusco, L. Pratesi, M. Bragoni, P. Coiro, M. Multari, V. Venturiero, D. De Angelis, and S. Paolucci, Effects of walking endurance reduction on gait stability in patients with stroke, *Stroke Res. Treatment*, article ID 810415, p. 6, 2012.

[39] N. M. Salbach, S.J.T. Guilcher, and S. B. Jaglal, "Physical therapists' perceptions and use of standardized assessments of walking ability post-stroke," *J. Rehabil, Med.*, vol. 43, no. 6, pp. 543–549, May 2011.

[40] W. H. Wu, A. A. Bui, M. A. Batalin, D. Liu, and W. J. Kaiser, "Incremental diagnosis method for intelligent wearable sensor systems," *IEEE Trans. Inf. Technol. Biomed.*, vol. 11, no. 5, pp. 553–562, Sep. 2007.

Yinlai Jiang received the PhD degree in engineering from Kochi University of Technology, Japan, in 2008. He was a research associate in the Kochi University of Technology from 2008 to 2012. He is currently an assistant professor in the Research Institute, Kochi University of Technology. His current research interests include visual cognition, medical and biological engineering, and computational intelligence. He is a member of the IEEE.

Isao Hayashi received the PhD degree in engineering from Hannan University in 1991. He worked as a researcher in Sharp Corporation from 1981 to 1983, and Panasonic Corporation from 1987 to 1993. He was with Hannan University first as an assistant professor from 1993 to 1994, then an associate professor from 1994 to 1997, and finally as a professor from 1997 to 2004. He has been a professor in the Faculty of Informatics, Kansai University, since 2004. His current research interests include visual cognition, embodied knowledge, and motion analysis. He is a member of the IEEE.

Shuoyu Wang received the PhD degree in electrical engineering from Hokkaido University, Japan, in 1993. He was an assistant professor in the Department of Electronic Information Engineering, Yamagata University, from 1993 to 1997, and an associate professor in the Department of Intelligent Mechanical Systems Engineering, Kochi University of Technology, from 1997 to 2002. Since January 2002, he has been a professor in the Department of Intelligent Mechanical Systems Engineering, Kochi University of Technology. His current research interests include walking rehabilitation robots, control, and fuzzy reasoning. He is a member of the IEEE.